An Optimization Method for Designing Large PV Plants

Tamas Kerekes, *Member, IEEE*, Eftichis Koutroulis, *Member, IEEE*, Dezső Séra, *Member, IEEE*,
Remus Teodorescu, *Fellow, IEEE*, and Markos Katsanevakis

Abstract—Large-scale photovoltaic (PV) plants enable the reduction of the PV plant cost per watt of nominal power that is installed. In this paper, a new method is presented for the calculation of the optimal configuration of large PV plants, such that the levelized cost of the generated electricity (LCOE) is minimized. The proposed design optimization process is performed by considering the impact of the number of components, as well as their type and arrangement within the installation field, on the tradeoff between the lifetime cost and the corresponding energy production of the PV plant. The high-accuracy feature of the energy production calculations that are performed by the proposed design tool has been validated using experimental operational data of an existing PV plant. The design results demonstrate that using the proposed optimization method allows a reduction of the cost of the energy that is generated by the large-scale PV plant, thus enabling the maximization of the economic benefit that is obtained during the operational lifetime period of the PV system.

Index Terms—Design optimization, genetic algorithms, grid connected, levelized cost of energy, photovoltaic (PV) systems.

Nomenclature

$A_{s,I}$	Shaded area of each photovoltaic (PV) set.
BOS	Total capital cost increment due to the balance-of-system components.
C_B	Manufacturing and installation cost of the PV modules mounting structures.
C_c	Total capital cost of the PV plant.
$C_{c,ac}$	Cost of the ac cables.
$C_{c,dc}$	Cost of the dc cables.
C_{IC}	Cost of the PV plant to MV PCC interconnection cable.
C_{INV}	Price of each dc/ac inverter.
$C_{i/t}$	Cost of the interconnection transformer.
C_L	Cost of purchasing the required installation area.
C_m	Present value of the total maintenance cost during the PV plant operational lifetime period.
C_{PV}	Price of each PV module.
D_{PCC}	Distance of the PV plant to the MV PCC.
DIM_1	Actual length of the southern side of the available installation area.

$DIM_{1,max}$	Maximum permissible length of the southern side of the available installation area.
E_{tot}	Total energy actually injected into the electric grid by the PV plant during its operational lifetime.
EAF	Energy availability factor of the PV plant.
F_y	Distance between adjacent PV blocks.
G	Solar irradiance incident on the PV module surface.
$L_{pv,1}$	Length of each PV module.
$L_{pv,2}$	Width of each PV module.
LCOE	Levelized cost of the generated electricity.
$M_{c,ac}$	Annual maintenance cost of the ac cables.
$M_{c,dc}$	Annual maintenance cost of the dc cables.
M_{IC}	Annual maintenance cost of the interconnection cables.
M_{INV}	Annual maintenance cost of the dc/ac inverters.
$M_{i/t}$	Annual maintenance cost of the interconnection transformer.
M_{PV}	Annual maintenance cost of the PV modules.
$N_{I,o}$	Total number of PV modules in the PV plant.
N_i	Total number of dc/ac inverters in the PV plant.
N_p	Parallel-connected PV strings per PV set.
N_r	Number of rows of PV sets per block.
N_s	Number of series connected PV modules per PV string.
N_{smax}	Maximum number of PV modules which can be connected in series in each PV string.
N_{smin}	Minimum number of PV modules which can be connected in series in each PV string.
$P_{grid,max}$	Maximum power which can be injected by the PV plant to the electric grid.
P_{in}	Output power of each PV set.
$P_{i,na}$	Maximum permissible operating power level of each dc/ac inverter.
$P_{i,sc}$	Self-power consumption of each dc/ac inverter.
$P_{M,STC}$	PV module power rating.
P_m	MPP power of each PV module.
P_{m_sh}	MPP power of the PV module after shading.
P_o	Total output power of each dc/ac inverter.
P_{plant}	PV plant total power injected into the grid.
$P_{plant,nom}$	PV plant power rating.
P_{pv}	Actual output power of each PV module.
PL_{ac}	Power-length product of ac cables from the dc/ac inverters to the interconnection transformer.
PL_{DC}	Power-length product of dc cables from PV modules to dc/ac inverters.
R	Resistance of the electric grid.
R_{PV}	Residual-value coefficient of the PV modules.
R_{TC}	Present value of the dc/ac inverters repair cost.

$S_g(y)$	Annual growth of the maximum power which can be injected by the PV plant to the electric grid.
S_p	Percentage of the PV module total area shaded by surrounding obstacles.
SIF	Shade impact factor.
T_A	Ambient temperature.
U_n	Medium-voltage nominal level.
$V_{DC,max}$	PV inverter maximum permissible dc input voltage.
$V_{i,max}$	PV inverter dc input maximum MPP voltage.
$V_{M,max}$	PV module maximum MPP voltage.
$V_{oc,max}$	PV module maximum open-circuit voltage.
$\mathbf{X}$	Vector of the decision variables.
c_f	Dimensionless factor of the PV modules purchase cost.
d	Day number ($1 \leq d \leq 365$).
d_f	PV module power derating factor due to dirt.
d_i	Nominal annual discount rate.
g	Annual inflation rate.
k	Per-unit maximum permitted voltage change.
n	PV plant operational lifetime.
$n_{l,ac}$	Power loss coefficient of the ac cables.
$n_{l,dc}$	Power loss coefficient of the dc cables.
$n_{l,i/c}$	Power loss coefficient of the PV plant to MV PCC interconnection cable.
n_{PV}	PV modules lifetime.
$r(y)$	PV module power annual reduction coefficient.
s	Capital subsidization rate.
t	Time number ($1 \leq t \leq 24$).
t_1	Hour of the day the obstacles start to cause shadow.
t_2	Time duration of the shadow effect.
y	Year number ($1 \leq y \leq n$).
Δt	Simulation time step.
β	PV modules tilt angle.
η_{inv}	dc/ac inverter power conversion efficiency.
η_{mppt}	dc/ac inverter maximum power point tracking (MPPT) efficiency.
η_t	Interconnection transformer efficiency.

I. INTRODUCTION

DURING 2011, there were 27.7 GW of new photovoltaic (PV) systems installed worldwide, which ranged from kilowatts up to several tens of megawatts in size. There are now six countries where more than 1 GW of PV has been installed in 2011, compared with only three during 2010. In 2011, Italy led the market, which was followed by Germany, China, the U.S., France, and Japan. Europe is still the major player on the PV market with a 75% share of all new capacities. There are now 67.4 GW of PV systems installed worldwide, which means that PV is the third renewable energy technology after hydro and wind [1]. Special focus is given to large-scale PV plants (i.e., >200 kW nominal power rating—the biggest plants reaching several tens of MW of capacity), since they enable the reduction of the PV plant cost per watt of nominal power that is installed [2]–[4]. Toward this direction, various new dc/ac inverter configurations have been introduced recently, which

target facilitation of the efficient and cost-effective operation of large PV plants [5]–[9].

Large-scale PV plants are composed of several thousands of PV panels, each being in the range of 150–350 W. During the design of a large PV plant, the designer has to select the values of many design parameters: number and type of PV modules and PV inverters, distribution of the components in the installation field, etc. Additionally, the values of the design parameters are conflicting. For example, the installation of many PV modules increases the PV plant energy production but also leads to high-installation and lifetime maintenance cost of the PV plant. Thus, the design of a large PV plant is a big challenge.

The process to configure a large PV plant is typically performed by taking into consideration not only the cost of the installation, but also the annual energy production (AEP), the performance ratio (PR), and/or the levelized cost of generated electricity (LCOE). AEP is equal to the aggregate energy injected into the electric grid during a one-year period that the PV plant is servicing [10]. PR quantifies the overall effect of losses, and it is equal to the ratio of the final PV system yield divided by the reference yield [11]. LCOE is a metric that is used in the electricity market in order to evaluate the commercial break-even of alternative energy technologies [12]. LCOE takes into account the electrical output of the installation over its lifetime, and it is usually expressed in € /MWh.

A decision support tool to optimally plan large-scale PV generation investments is presented in [13]. The optimal values of the PV plant location, size, and time of investment, which comprise the optimization problem decision variables, are calculated such that the net present value of the investor's profit is maximized. The financial analysis of a large-scale PV plant is presented in [14]. The analysis is performed by calculating the expected power generation of the PV plant using an appropriate model of the PV modules and considering the capital investment cost, the annual operating and maintenance costs, and the performance derating factor of the PV system. Also, the internal rate of return and payback time period are used as metrics in order to explore the profitability of the PV installation.

The power rating of the step-up transformers that are employed in large-scale PV plants is calculated in [15], such that the economic benefit that is obtained during the PV plant lifetime is maximized. Both the cost of energy losses due to transformer overloads and efficiency and the capital and lifetime operating costs of the transformer are considered during the design process. The impact of energy losses due to grid instability is also taken into account.

An analytic hierarchy process is proposed in [16] for the selection of the optimal manufacturing technology of PV modules (i.e., multicrystalline silicon, CdTe etc.) that are employed in large-scale PV systems. The decision-making process is based on criteria such as the investment cost, energy production, CO_2 emission, and energy payback time. The impact of the PV modules' configuration (i.e., connection in series and/or parallel) on the PV array power production under partial shading conditions is explored in [17]. A tradeoff study is presented in [18], which evaluates the benefits of using a distributed PV architecture as compared with the central inverter structures in large-scale PV

plants. The effects of partial shading, PV module mismatch, cable losses, and power converter efficiency are also quantified in order to obtain the energy yield of the PV plant for each of the architectures under study. The optimum relation between the PV array nominal power rating and the dc/ac inverter nominal ac power capacity as a function of the solar irradiation conditions and the PV array surface tilt and azimuth, which results in the minimization of the energy production losses due to inverter output power limitation, is explored in [19]. A cost analysis, together with an investigation of the impact of time threshold, which is defined as the protection time delay when the input power of the inverter is 150% of its nominal power, is additionally presented in [20].

A sizing algorithm that uses evolutionary programming is proposed in [21] for the design of roof-mounted grid-connected PV systems. The optimal type of PV modules and dc/ac inverter are calculated such that the expected annual specific yield of the PV system is maximized. In [22], the optimal tilt of the PV modules, number of collector rows installed in the PV field, and distance between the rows are calculated such that PV plant energy production is maximized.

In this paper, a new method is presented for the optimal design of large-scale PV plants. Using the proposed optimization technique, the optimal configuration of the large PV plant is calculated, such that the LCOE is minimized. The design process is performed by considering the impact of the components' number, type (in terms of their operational characteristics, such as the power rating, the operating voltage range etc.), and arrangement within the installation field on the tradeoff between the lifetime cost and the corresponding energy production of the PV plant. In contrast with the past-proposed methods that are described previously, the optimization method presented in this paper has the advantage that it takes into account during the design flow simultaneously all design characteristics of large PV plants, which highly affect both the resulting energy production and the capital and lifetime maintenance costs, such as the arrangement of the PV arrays within the installation field, the reduction of the power produced by the PV plant due to mutual shading between adjacent rows of PV modules, etc.

This paper is organized as follows. The large PV plant modeling and the proposed optimization algorithm are analyzed in Section II. The results of a design example are discussed in Section III and finally the conclusions are presented.

II. PROPOSED OPTIMIZATION METHOD

A. Modeling of the Large PV Plant

A block diagram of the large PV plant that is considered in the proposed optimization process is illustrated in Fig. 1. The PV modules are distributed in multiple PV inverters, and the generated power is injected into the electric grid at the point of common coupling (PCC) through an interconnection (i/c) transformer and cable, respectively.

The total number of PV modules which must be installed in the PV plant $N_{I,o}$ is calculated according to the PV plant power rating $P_{\text{plant,nom}}(\text{MW}_p)$ that is specified by the PV plant
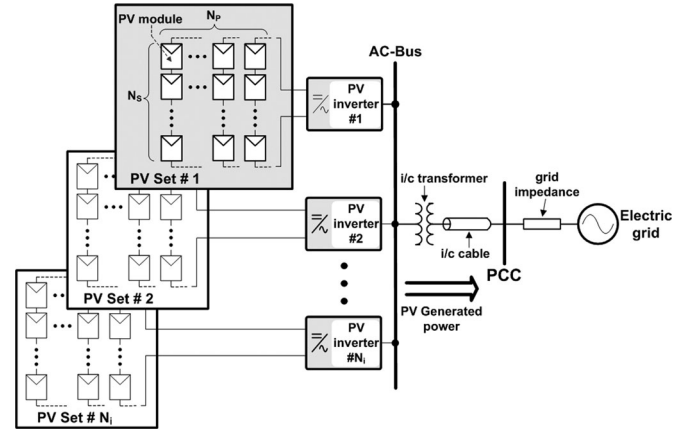

Fig. 1. Block diagram of the large PV plant.

designer, as follows:

$$N_{I,o} = \frac{P_{\text{plant,nom}} \cdot 10^6}{P_{M,\text{STC}}} \qquad (1)$$

where $P_{M,\text{STC}}$ (W) is the power rating of each PV module.

As shown in Fig. 1, the PV modules of the PV plant are distributed in PV sets, and each PV set is connected to a PV inverter. Each PV set consists of N_p PV strings ($N_p \geq 1$), while each string is comprised of N_s PV modules that are connected in series ($N_s \geq 1$). The minimum and the maximum number of PV modules which can be connected in series in each PV string, $N_{s\min}$ and $N_{s\max}$, respectively, are calculated according to the PV inverter dc input maximum power point (MPP) voltage level $V_{i,\max}$ (V) and the maximum permissible dc input voltage level, $V_{\text{DC,max}}$ (V), both specified by the PV inverter manufacturer, as follows:

$$N_{s\min} = 1 \leq N_s \leq N_{s\max} =$$
$$= \min\left[\text{floor}\left(\frac{V_{i,\max}}{V_{M,\max}}\right), \text{floor}\left(\frac{V_{\text{DC,max}}}{V_{\text{oc,max}}}\right)\right] \quad (2)$$

where $V_{\text{oc,max}}$ and $V_{M,\max}$ are the maximum open-circuit voltage (V) and MPP voltage (V), respectively, which can be developed at the PV module output terminals according to the incident solar irradiation and ambient temperature conditions that prevail at the PV plant installation site during the year.

The actual output power of each PV module on year y ($1 \leq y \leq n$), day d ($1 \leq d \leq 365$), and at time t ($1 \leq t \leq 24$), $P_{\text{pv}}(y,d,t,\beta)$ (kW) is calculated according to the following equation [23]:

$$P_{\text{pv}}(y,d,t,\beta) = \left[1 - y \cdot \frac{r(y)}{100}\right] \cdot \left(1 - \frac{d_f}{100}\right) \cdot P_{m\_\text{sh}}(y,d,t,\beta) \qquad (3)$$

where β (°) is the PV modules tilt angle ($0^o \leq \beta \leq 90^o$), $r(y)$ (%/year) is the annual reduction coefficient of the PV module output power (if $y = 1$, then $r(y) = 0$; for $1 < y \leq n$, its value is specified by the PV module manufacturer), d_f (%) is the PV module output power derating factor due to the dirt that is deposited on its surface (derating up to 6.9% has been reported for large-scale PV plants in [24]), and $P_{m\_\text{sh}}(y,d,t,\beta)$ (kW) is

the output power of each PV module at the MPP [25], which is calculated also considering the shading conditions as analyzed next.

Although large-scale PV plants are typically built such that there are no obstacles surrounding the installation field, the impact to the PV plant power production of topographies where a uniform shadow is projected by such objects on all cells of the PV module has also been incorporated in the proposed design method. The PV plant designer specifies the percentage of the PV module total area that is shadowed by the surrounding obstacles S_p (%) as well as the hour of the day t_1 (h) that these obstacles start to shadow the PV modules of the PV plant and the corresponding time duration of the shadow t_2 (h). Then, the output power of each PV module is calculated considering that for the cases under study, the power loss due to shading is proportional to the shaded area of the PV module [26], as follows:

$$
\begin{aligned}
&P_{m\_\mathrm{sh}}(y,d,t,\beta) \\
&= \begin{cases} \left(1 - \dfrac{S_p}{100}\right) \cdot P_m(y,d,t,\beta), & \text{if } t_1 \le t \le t_1 + t_2 \\ P_m(y,d,t,\beta), & \text{else.} \end{cases}
\end{aligned}
\tag{4}
$$

where $P_m(y,d,t,\beta)$ (W) is the power that is produced by each PV module at the MPP.

The value of S_p in (4) is estimated using field measurements or geometrical calculations. The value of $P_m(y,d,t,\beta)$ is calculated as analyzed in [27] using the specifications of the PV module under standard test conditions (STC), available in the datasheet that is provided by their manufacturer, as well as the solar irradiance $G(d,t,\beta)$ (kW/m^2) incident on a PV module with a tilt angle equal to β (°) and the ambient temperature conditions $T_A(d,t)$ (°C), respectively, during day d ($1 \le d \le 365$) and at time t ($1 \le t \le 24$).

The output power of each PV set (i.e., dc input power of each inverter) is calculated also incorporating the impact of mutual shading between adjacent PV blocks on the resulting power production, according to the model for the power loss due to shading that is presented in [26], as follows:

$$
\begin{aligned}
P_{\mathrm{in}}(q) &= \left[1 - \frac{A_{s,I}(q)}{N_s \cdot N_p \cdot L_{\mathrm{pv},1} \cdot L_{\mathrm{pv},2}} \cdot \mathrm{SIF}\right] \cdot \\
&\quad \times \left(1 - \frac{n_{l,\mathrm{dc}}}{100} \cdot \mathrm{PL}_{\mathrm{dc}}\right) \cdot N_s \cdot N_p \cdot \\
&\quad \eta_{\mathrm{mppt}}(N_s \cdot N_p \cdot P_{\mathrm{pv}}(y,d,t,\beta)) \cdot P_{\mathrm{pv}}(y,d,t,\beta)
\end{aligned}
\tag{5}
$$

where $A_{s,I}(q)$ (m^2) is the shaded area of PV set q which is caused due to shading by the front (southern) PV block, $L_{\mathrm{pv},1}$ and $L_{\mathrm{pv},2}$ (m) are the length and width of each PV module, $\mathrm{SIF} = 2$ is the shade impact factor [26], $n_{l,\mathrm{dc}}$ is the dc cables power loss coefficient ($\%/kW/m$), $\mathrm{PL}_{\mathrm{DC}}$ is the power-length product ($kW_p \cdot m$) of dc cables from PV modules to dc/ac inverters in the PV plant, and η_{mppt} is the MPPT efficiency of the dc/ac inverters.

The value of $A_{s,I}(q)$ is calculated geometrically by using the relative position of consecutive blocks of PV sets (e.g., blocks #1 and #2, respectively, in Fig. 2) within the installation area. For the PV sets that comprise the southernmost block, it holds
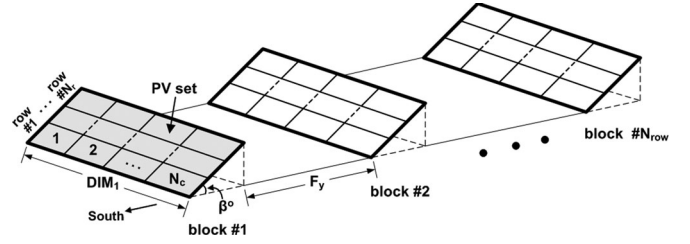

Fig. 2. Arrangement of the PV power generation sets in blocks within the available installation area and the PV power generation sets in rows within each block.

that $A_{s,I}(q) = 0$. Using this method, the proposed algorithm is able to detect the overall optimal distance of adjacent PV blocks even if during some time intervals, one or more of them are mutually shaded. Thus, it is possible to explore the impact of the PV plant configuration on the energy-production/land-cost tradeoff.

The total output power of each dc/ac inverter $P_o(q)$ (MW) at day d ($1 \le d \le 365$), and at time t ($1 \le t \le 24$) is calculated as follows:
1) if $P_{\mathrm{in}}(q) \le P_{i,na}$, then $P_o(q) = \eta_{\mathrm{inv}}(P_{\mathrm{in}}(q)) \cdot P_{\mathrm{in}}(q)$, else $P_o(q) = \eta_{\mathrm{inv}}(P_{i,na}) \cdot P_{i,na}$;
2) if $P_{\mathrm{in}}(q) < P_{i,\mathrm{sc}}$ or $N_s \cdot V_M(y,d,t,\beta) < V_{i,\min}$, then $P_o(q) = 0$

where $P_{i,na}$ (kW) is the PV inverter maximum permissible operating power level, which is provided by the manufacturer of the dc/ac inverter as a function of the installation altitude and ambient temperature, $P_{i,\mathrm{sc}}$ (kW) is the self-power consumption during operation (it is equivalent to the minimum required dc power for operation) of each dc/ac inverter, provided by the manufacturer of the dc/ac inverter, $V_M(y,d,t,\beta)$ (V) is the MPP voltage of the PV modules on year y ($1 \le y \le n$), day d ($1 \le d \le 365$) and at time t ($1 \le t \le 24$), which is calculated as analyzed in [27], and $V_{i,\min}$ (V) is the PV inverter dc input minimum permissible MPP voltage level.

Both the dc/ac inverter MPPT efficiency in (5) η_{mppt} and the power conversion efficiency above η_{inv} are stored in the form of a look-up table of the efficiency value versus the corresponding PV set output power.

As illustrated in Fig. 2, the PV power generation sets are arranged within the available installation area in multiple blocks, where each block is comprised of multiple rows of PV generation sets. The number of rows of PV modules sets per block is equal to N_r. The adjacent blocks are installed with a distance F_y (in meters, $F_y \ge 0$) between them, which defines the shading conditions of each block, as described previously. The PV modules tilt angle β (°) is constant during the year. The length of the southern side of the available installation area DIM_1 (m) is constrained to be less than the maximum permissible length, which is specified by the PV plant designer $\mathrm{DIM}_{1,\max}$ (m), such that

$$\mathrm{DIM}_1 \le \mathrm{DIM}_{1,\max}. \tag{6}$$

The parameters β, N_r, F_y, and DIM_1 are design variables, and their optimal values are calculated by the optimization algorithm.

The total power that the PV plant is able to inject into the electric grid $P_{\text{plant}}(y, d, t, \beta)$ (MW) at day d ($1 \leq d \leq 365$) and at time t ($1 \leq t \leq 24$) is given by

$$P_{\text{plant}}(y, d, t, \beta) = \frac{\frac{\eta_t}{100} \cdot \left(1 - \frac{n_{l,\text{ac}}}{100} \cdot \text{PL}_{\text{ac}}\right)}{1000} \cdot$$
$$\times \left(1 - \frac{n_{l,i/c}}{100} \cdot \text{PL}_{I/C}\right) \cdot \sum_{q=1}^{N_i} P_o(q). \quad (7)$$

where η_t (%) is the efficiency of the interconnection transformer, PL_{ac} is the power-length product ($kW_p \cdot m$) of ac cables from the dc/ac inverters to the interconnection transformer, $N_i = N_{I,o}/(N_s \cdot N_p)$ is the total number of dc/ac inverters that are used in the PV plant, $n_{l,\text{ac}}$ is the power loss coefficient of the ac cables ($\%/kW/m$), and $n_{l,i/c}$ is the power loss coefficient of the PV plant to medium-voltage (MV) PCC interconnection cable ($\%/MW/m$).

However, depending on its operating conditions (e.g., maintenance, low load, etc.), the grid might not be able to absorb the generated power. Thus, in case that $P_{\text{plant}}(y, d, t, \beta) > P_{\text{grid,max}}(y, d, t) \cdot [1 + (y - 1) \cdot \frac{S_g(y)}{100}]$, then

$$P_{\text{plant}}(y, d, t, \beta) = P_{\text{grid,max}}(y, d, t) \cdot \left[1 + (y - 1) \cdot \frac{S_g(y)}{100}\right] \quad (8)$$

where $P_{\text{grid,max}}(y, d, t)$ (MW) is the maximum power that can be injected by the PV plant to the electric grid at day d ($1 \leq d \leq 365$) and at time t ($1 \leq t \leq 24$) of year y ($1 < y \leq n$), including programmed maintenance and grid limitations, and $S_g(y)$ (%) is the annual growth of the maximum power which can be injected by the PV plant to the electric grid due to the increase of the grid load and the grid capacity.

Additionally, the maximum power which can be injected by the PV plant, such that the voltage change is limited to the maximum permitted level, $k \cdot U_n$ (e.g., $k = \pm 0.1$ per unit), is given by

$$P_{\text{plant}}(y, d, t, \beta) \leq k \cdot \frac{U_n^2}{\left(R + \frac{n_{l,i/c}}{100} \cdot U_n^2 \cdot D_{\text{PCC}} \cdot 10^{-6}\right)}$$
$$= P_{\text{plant,max}} \quad (9)$$

where U_n is the MV nominal voltage level, D_{PCC} (m) is the distance of the PV plant to the MV PCC, and R (Ω) is the resistance of the electric grid.

In case that the calculated value of $P_{\text{plant}}(y, d, t, \beta)$ is such that $P_{\text{plant}}(y, d, t, \beta) > P_{\text{plant,max}}$, then the dc/ac inverters output power is limited such that $P_{\text{plant}}(y, d, t, \beta) = P_{\text{plant,max}}$.

The total energy that is actually injected into the electric grid by the PV plant during its operational lifetime E_{tot} (MWh) is given by

$$E_{\text{tot}} = \frac{\text{EAF}}{100} \cdot \sum_{y=1}^{n} \sum_{d=1}^{365} \sum_{t=1}^{24} P_{\text{plant}}(y, d, t, \beta) \cdot \Delta t \quad (10)$$

where EAF (%) is the energy availability factor of the PV plant due to scheduled and nonscheduled maintenance events of the PV plant components, such as the PV modules, the dc/ac

inverters etc. (typically, EAF $> 99.5\%$) [28] and $\Delta t = 1\,h$ is the simulation time step.

The total capital cost of the PV plant $C_c(\mathbf{X})$ (€) is calculated as follows:

$$C_c(\mathbf{X}) = \left(1 - \frac{s}{100}\right) \cdot \left(1 + \frac{\text{BOS}}{100}\right) \cdot [N_i \cdot N_s \cdot N_p$$
$$\cdot \frac{P_{M,\text{STC}}}{1000} \cdot \left(1 - \frac{R_{\text{PV}}}{100}\right) \cdot C_{\text{PV}} + N_i \cdot P_{i,n} \cdot C_{\text{INV}}$$
$$+ C_L + C_B + C_{i/t} + C_{c,\text{dc}} + C_{c,\text{ac}} + C_{\text{IC}}] \quad (11)$$

where $\mathbf{X} = [N_s, N_p, N_r, F_y, \beta, \text{DIM}_1]$ is the vector of the decision variables of the large PV plant design process, s (%) is the capital subsidization rate, BOS (%) is the PV plant total capital cost increment due to the balance-of-system components (e.g., switchgears, junction boxes, land preparation cost, system design, construction management, project engineering, end of life dismantlement costs etc.) used to build the PV plant [29], C_{PV} (€/kW_p) and C_{INV} (€/kW_p) are the prices of each PV module and dc/ac inverter, respectively, R_{PV} is the residual-value coefficient of the PV modules (%), C_L (€) is the cost of purchasing the required installation area, C_B (€) is the manufacturing and installation cost of the PV modules mounting structures, $C_{i/t}$ is the cost of the interconnection transformer (€), $C_{c,\text{dc}}$ is the cost of the dc cables (€), $C_{c,\text{ac}}$ is the cost of the ac cables (€), and C_{IC} (€) is the cost of the PV plant to MV PCC interconnection cable.

In (11), the residual-value coefficient of the PV modules R_{PV} (%) is calculated assuming that the salvage value of the PV modules is proportional to their remaining life:

$$R_{\text{PV}} = c_f \cdot \left[1 - n \cdot \frac{r(n)}{100}\right] \cdot \frac{n_{\text{PV}} - n}{n_{\text{PV}}} \cdot 100 \quad (12)$$

where c_f is a dimensionless factor, which is used in order to take into account that the purchase cost of the PV modules at the nth year will be different compared with its present value (due to e.g., inflation, taxation etc.), and n_{PV} is the PV modules' lifetime (years), which is specified by their manufacturer.

The present value of the total maintenance cost $C_m(\mathbf{X})$ (€) during the PV plant operational lifetime period is calculated using the following equation:

$$C_m(\mathbf{X}) = \left(N_i \cdot N_s \cdot N_p \cdot \frac{P_{M,\text{STC}}}{1000} \cdot M_{\text{PV}} + N_i \cdot P_{i,n} \cdot M_{\text{INV}}\right.$$
$$\left. + M_{i/t} + M_{c,\text{dc}} + M_{c,\text{ac}} + M_{\text{IC}}\right)$$
$$\cdot \left(1 + \frac{g}{100}\right) \cdot \frac{1 - \left(\frac{1 + \frac{g}{100}}{1 + \frac{d_i}{100}}\right)^n}{\frac{d_i - g}{100}} + R_{TC} \quad (13)$$

where M_{PV} are M_{INV} (€/kW_p) are the annual maintenance costs of the PV modules and the dc/ac inverters, respectively, $M_{i/t}$ (€) is the annual maintenance cost of the interconnection transformer, $M_{c,\text{dc}}, M_{c,\text{ac}}$, and M_{IC} (€) are the annual maintenance costs of the dc, ac, and interconnection cables, respectively, g (%) is the annual inflation rate, d_i (%) is the nominal
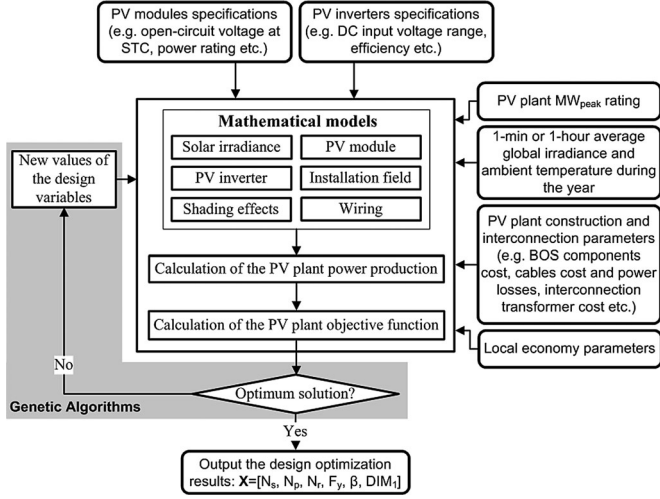
Fig. 3. Flowchart of the proposed optimization process.

annual discount rate, and R_{TC} (€) is the present value of the total cost of repairing the dc/ac inverters of the PV plant.

The value of R_{TC} in (13) is calculated according to the mean time between failures (MTBF) of the dc/ac inverters, which are specified by the manufacturer, as analyzed in [30].

The hourly average values of solar irradiation and ambient temperature conditions during the year, as well as the values of $P_{\text{plant,nom}}, P_{M,\text{STC}}, V_{i,\min}, V_{i,\max}, V_{\text{DC,max}}, r(\cdot), d_f, L_{\text{pv},1}, L_{\text{pv},2}, S_p, t_1, t_2, n_{l,\text{dc}}, \text{PL}_{\text{DC}}, \eta_{\text{mppt}}, \eta_{\text{inv}}, P_{i,na}, P_{i,\text{sc}}, DIM_{1,\max}, \eta_t, n_{l,\text{ac}}, n_{l,i/c}, S_g(\cdot), k, U_n, D_{\text{PCC}}, R, \text{EAF}, s,$ BOS, $C_{\text{PV}}, C_{\text{INV}}, C_L, C_B, C_{i/t}, C_{c,\text{dc}}, C_{c,\text{ac}}, C_{\text{IC}}, c_f, n_{\text{PV}}, M_{\text{PV}}, M_{\text{INV}}, M_{i/t}, M_{c,\text{dc}}, M_{c,\text{ac}}, M_{\text{IC}}, g,$ and d_i are input in the model of the large PV plant that is presented in this section, which is comprised of (1)–(13), by the designer of the PV plant at the beginning of the proposed optimization process. This model is used by the optimization algorithm in order to calculate the optimal configuration of the PV plant, as analyzed in the following paragraph.

B. Optimization Algorithm

In the proposed methodology, the design variables whose optimal values are calculated by the optimization algorithm are the parameters N_s and N_p, the number of rows of PV modules sets per block N_r, the distance between adjacent blocks F_y, the tilt angle β (°), and the length of the southern side of the installation area DIM_1 (m). Any other design variable of the PV plant [e.g., N_c and N_{row} in Fig. 2, N_i in (7) etc.] can be calculated using these parameters as a reference.

The flowchart of the proposed optimization process is depicted in Fig. 3. For each combination of PV module and PV inverter types and operational specifications input by the PV plant designer, a set of design variable values is generated by the optimization algorithm. Using these values, the mathematical models of the large PV plant components that are presented in Section II-A are evaluated, in order to calculate the corresponding value of the optimization process objective function. The objective function that is considered in the proposed op-

timization procedure is the LCOE [12], which is calculated as the ratio of the present value of the total life cycle costs of the PV plant, divided by the total energy produced over its lifetime period:

$$\underset{\mathbf{X}}{\text{minimize}} \{\text{LCOE}(X)\} = \underset{\mathbf{X}}{\text{minimize}} \left\{ \frac{C_c(\mathbf{X}) + C_m(\mathbf{X})}{E_{\text{tot}}(\mathbf{X})} \right\}$$

subject to: design constraints are met   (14)

where $\mathbf{X} = [N_s, N_p, N_r, F_y, \beta, \text{DIM}_1]$ is the vector of the decision (design) variables.

The LCOE is used as the objective function in the proposed optimization process, since it enables to derive the most cost-effective configuration of the large-scale PV plant during its operational lifetime period. The values of $C_c(\mathbf{X}), C_m(\mathbf{X})$, and $E_{\text{tot}}(\mathbf{X})$ in (14) are calculated using (10), (11), and (13), respectively. The design constraints are expressed by all inequalities setting the upper and lower permissible values of the optimization problem design variables, such as (2), (6), etc. For the LCOE calculation in (14), the economic value of the electric energy has been assumed constant during the operational lifetime period of the PV system, in order to decouple the optimization procedure from factors which are not relevant to the PV plant design process, such as state energy policies, unpredictable market conditions, etc.

New sets of the design variable values are iteratively generated by the optimization algorithm, and the aforementioned process is repeated until the optimum solution (i.e., the set of the large PV plant design variables), which results in the minimum LCOE value, has been derived. In the proposed design process, the genetic algorithms (GAs) are used to search for the optimal values of the design variables that are included in the vector X, which minimize the PV plant LCOE, since they have the ability to derive the global optimum solution with relative computational simplicity, even in the case of complicated problems with nonlinear cost functions or nonlinear constraints [31].

III. DESIGN EXAMPLE

The proposed methodology has been implemented in the form of a software program that is developed using the MATLAB platform and the GA functions that are available in the library of the Global Optimization Toolbox.

Initially, the accuracy of the energy production calculations that are performed by the proposed design tool, which have been described in Section II, was evaluated using the experimentally measured operational data of a $40\,kW_p$ PV plant that is installed in Nordsømøllen (Denmark) as a reference. The technical and economical parameters of the Nordsømøllen PV plant are summarized in Tables I and II, respectively. The prefixed design parameters of this PV plant are $N_s = 13, N_p = 8, N_r = 1, F_y = 0, \beta = 30°$, and $\text{DIM}_1 = 46.8\,m$. Also, an obstacle that exists besides the PV array of the Nordsømøllen PV plant causes shadowing with $S_p = 20\%$ on the PV modules during the time period 06:00–09:00 A.M. These data, as well as the technical and economical parameters of the Nordsømøllen PV plant that are summarized in Tables I and II, were input in both the mathematical models that are used by the proposed

TABLE I
TECHNICAL CHARACTERISTICS OF THE NORDSØMØLLEN PV PLANT

Parameter	Value
Installed power	40 kW$_p$
Tilt angle	30º
Latitude / longitude	54.77º / 9.38º
PV modules	312 x Sharp NT-L7E4EZ ($P_m = 127$W, $V_M = 26.7$V under Standard Test Conditions)
DC/AC inverters	3 x Danfoss TLX 15k

TABLE II
ECONOMICAL PARAMETERS OF THE NORDSØMØLLEN PV PLANT

PV modules	
Cost (module, mounting, wiring, transport, etc.)	3295.84 €/ kW$_p$
Annual maintenance cost	32.96 €/ kW$_p$
DC/AC inverter	
Cost	266 €/kW
Annual maintenance cost	2.66 €/kW
Repair cost	3.99 €/kW
Other	
Installation land cost	1.97 €/ m^2
Feed in tariff	0.2323 €/kWh

TABLE III
MEASURED AND COMPUTED AEP OF THE NORDSØMØLLEN PV PLANT

	AEP (MWh)
Experimentally measured	39.591
PVSYST	37.619
Proposed design optimization tool	38.983

optimization algorithm, as well as the commercially available software PVSYST [32]. The values of AEP for the year 2009, which have been experimentally measured and calculated by each simulation tool, are presented in Table III. These energy production calculations have been performed by providing the 8760 experimentally measured hourly average values of solar irradiation and ambient temperature during the year, for the installation site of the Nordsømøllen PV plant, to the PV plant model that is presented in Section II. The AEP estimated by the proposed design optimization tool deviated from the experimentally measured value by only 1.54%, while PVSYST deviated by 4.98 %, thus indicating the high-accuracy feature of the calculations performed by the proposed design optimization tool.

In the next step, the proposed optimization algorithm was used for the design of a 1-MW large-scale PV plant in Nordsømøllen (Denmark) with $n = 25$ years, $g = 3$ %, $d_i = 5$ %, and $\text{DIM}_{1,\max} = 250$ m. The GA optimization process has been executed for 5000 generations with 70 chromosomes and 5 elite individuals in each generation, while the rest of the GA process parameters remained equal to their default values set in the corresponding MATLAB/Global Optimization Toolbox function. The optimal values of the design variables and LCOE are presented in Table IV. For comparison purposes, the
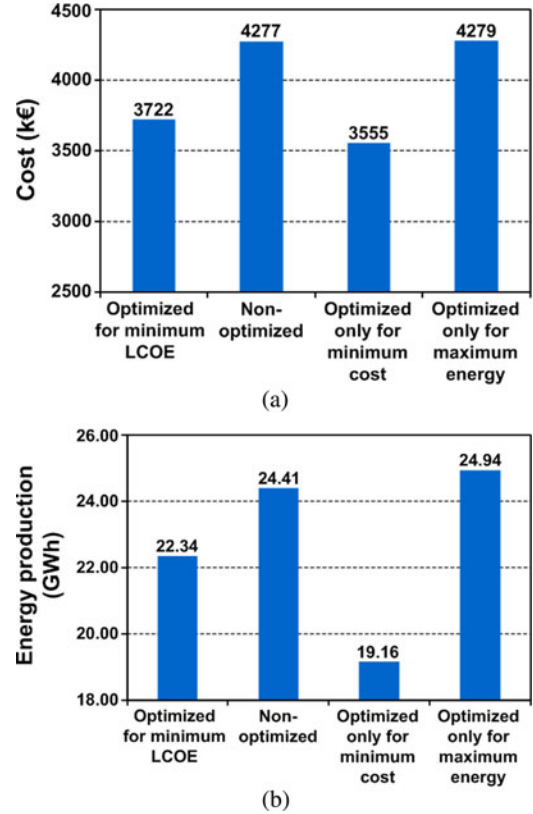

Fig. 4.   Performance of the optimized and nonoptimized 1-MW PV plants. (a) lifetime cost and (b) lifetime energy production.

configuration and LCOE of a nonoptimized 1-MW PV plant are also presented in Table IV. The nonoptimized PV plant is built by proportionally scaling the existing 40-kW PV system and applying an $F_y = 22$ m distance between adjacent PV blocks, such that any mutual shading results in less than 1% power loss during March–October. The LCOE of the optimized PV plant is lower by 4.9% compared with that of the nonoptimized PV plant.

The design optimization results for the cases where only the minimization of the lifetime cost or where only the maximization of the lifetime energy production of the 1 MW PV plant under study were used as objective functions in the design optimization process, are also presented in Table IV. It is observed that a different configuration of the PV plant is derived in each case. The value of LCOE resulting using the proposed design optimization technique is lower than that derived using the minimum-cost and maximum-energy objective functions by 10.2% and 2.9%, respectively.

The lifetime cost and energy production of the optimized and nonoptimized 1-MW PV plants are illustrated in Fig. 4(a) and (b), respectively. The lifetime cost of the PV plant that is designed using the proposed optimization method is lower by 13.0% compared with the cost of the nonoptimized and optimized for maximum energy PV systems, but it is higher by 4.7% compared with that of the PV plant that is optimized for minimum cost. The lifetime energy production of the minimum-LCOE PV plant is lower by 8.5% and 10.4% than the

TABLE IV
CONFIGURATION AND LCOE OF THE OPTIMIZED AND NONOPTIMIZED 1-MW PV PLANT

	N_s	N_p	N_r	F_y	β (°)	DIM_I (m)	LCOE (€/MWh)
Proposed method: optimized for minimum LCOE	18	8	7	7.5	35	207.9	166.6
Non-optimized	13	8	1	22	30	234.0	175.2
Optimized only for minimum cost	18	9	7	21.8	70	224.4	185.5
Optimized only for maximum energy	17	6	7	16.1	36	231.4	171.6

energy production of the nonoptimized and optimized for maximum energy PV systems, but it is higher by 16.6% than that of the minimum-cost PV plant. However, the PV plant configuration, which is derived using the proposed technique, achieves the lowest LCOE, as analyzed previously, thus guaranteeing the optimum performance of the large-scale PV plant in terms of the cost of the energy injected into the electric grid.

The successful calculation of the global optimum solution by the proposed GA-based procedure has been verified by also performing the PV plant design optimization process using an exhaustive search algorithm, where the objective function is evaluated for all combinations of the design variables values.

In this design example, a single type of components has been considered only in order to demonstrate the attributes of the proposed design technique. However, the optimal types of components (i.e., PV modules, dc/ac inverters etc.) can also be derived among various alternatives by executing the proposed optimization process for each of them and then selecting as the overall optimal configuration of the PV plant the output design variables (i.e., vector X) of the combination of component types that achieve the minimum LCOE.

IV. CONCLUSION

Large-scale PV plants enable the reduction of the PV plant cost per watt of nominal power that is installed. In this paper, a new method has been presented for the calculation of the optimal configuration of large PV plants, such that the LCOE is minimized. In contrast with the past-proposed methods applied to design large-scale PV systems, the proposed design optimization process is performed by considering the impact of the components number, type, and arrangement within the installation field on the tradeoff between the lifetime cost and the corresponding energy production of the PV plant.

The high-accuracy feature of the energy production calculations that are performed by the proposed design tool has been validated using experimental operational data of an existing PV plant at Nordsømøllen (Denmark). The design results demonstrate that using the proposed optimization method results in a reduction of the cost of the energy that is generated by the large-scale PV plant, thus enabling the maximization of the economic benefit that is obtained during the operational lifetime period of the PV system.

ACKNOWLEDGMENT

REFERENCES

[1] Market report 2011. (2012). Eur. Photovoltaic Industry Assoc. (EPIA). [Online]. Available: www.epia.org
[2] H. S. Krishnamoorthy, S. Essakiappan, P. N. Enjeti, R. S. Balog, and S. Ahmed, "A new multilevel converter for Megawatt scale solar photovoltaic utility integration," in *Proc. 27th Annu. IEEE Appl. Power Electron. Conf. Expo.*, 2012, pp. 1431–1438.
[3] J. Shi, W. Lee, Y. Liu, Y. Yang, and P. Wang, "Forecasting power output of photovoltaic systems based on weather classification and support vector machine," *IEEE Trans. Ind. Appl.*, vol. 48, no. 3, pp. 1064–1069, May/Jun. 2012.
[4] A. F. Panchula, W. W. Hayes, and A. A. Kimber, "First-year performance of a 20-MWac PV power plant," *IEEE J. Photovoltaics*, vol. 2, no. 3, pp. 359–363, Jul. 2012.
[5] T. Yoshino, R. Inzunza, T. Ambo, E. Ikawa, T. Takahashi, and N. Takahashi, "MW-range PCS for efficient operation of large PV plants," in *Proc. 3rd IEEE Int. Symp. Power Electron. Distrib. Gener. Syst.*, 2012, pp. 249–253.
[6] R. G. Wandhare and V. Agarwal, "Advance control scheme and operating modes for large capacity centralised PV-grid systems to overcome penetration issues," in *Proc. 37th IEEE Photovoltaic Spec. Conf.*, 2011, pp. 2466–2471.
[7] S. Rivera, B. Wu, S. Kouro, H. Wang, and D. Zhang, "Cascaded H-bridge multilevel converter topology and three-phase balance control for large scale photovoltaic systems," in *Proc. 3rd IEEE Int. Symp. Power Electron. Distrib. Gener. Syst.*, 2012, pp. 690–697.
[8] F. Spertino, F. Corona, and P. Di Leo, "Limits of advisability for master-slave configuration of DC-AC converters in photovoltaic systems," *IEEE J. Photovoltaics*, vol. 2, no. 4, pp. 547–554, Oct. 2012.
[9] W. Zhao, H. Choi, G. Konstantinou, M. Ciobotaru, and V. G. Agelidis, "Cascaded H-bridge multilevel converter for large-scale PV grid-integration with isolated DC-DC stage," in *Proc. 3rd IEEE Int. Symp. Power Electron. Distrib. Gener. Syst.*, 2012, pp. 849–856.
[10] A. Luque and S. Hegedus, *Handbook of Photovoltaic Science and Engineering*. New York: Wiley, 2003.
[11] A. Dolara, F. Grimaccia, S. Leva, M. Mussetta, R. Faranda, and M. Gualdoni, "Performance analysis of a single-axis tracking PV system," *IEEE J. Photovoltaics*, vol. 2, no. 4, pp. 524–531, Oct. 2012.
[12] M. Campbell, J. Blunden, E. Smeloff, and P. Aschenbrenner, "Minimizing utility-scale PV power plant LCOE through the use of high capacity factor configurations," in *Proc. 34th IEEE Photovoltaic Spec. Conf.*, 2009, pp. 421–426.
[13] W. Muneer, K. Bhattacharya, and C. A. Cañizares, "Large-scale solar PV investment models, tools, and analysis: The Ontario case," *IEEE Trans. Power Syst.*, vol. 26, no. 4, pp. 2547–2555, Nov. 2011.
[14] C.-H. Lin, W.-L. Hsieh, C.-S. Chen, C.-T. Hsu, T.-T. Ku, and C.-T. Tsai, "Financial analysis of a large-scale photovoltaic system and its impact on distribution feeders," *IEEE Trans. Ind. Appl.*, vol. 47, no. 4, pp. 1884–1891, Jul./Aug. 2011.

[15] A. Testa, S. De Caro, R. La Torre, and T. Scimone, "Optimal size selection of step-up transformers in PV plants," in *Proc. XIX Int. Conf. Electr. Mach.*, 2010, pp. 1–6.

[16] B. Yang, Y. Sun, and Y. Lin, "Decision-making on PV modules for very large scale photovoltaic systems using improved analytic hierarchy process," in *Proc. Asia-Pacific Power Energy Eng. Conf.*, 2011, pp. 1–5.

[17] X. Wu, X. Wei, T. Xie, and R. Yu, "Optimal design of structures of PV array in photovoltaic systems," in *Proc. Int. Conf. Intell. Syst. Design Eng. Appl.*, 2010, vol. 2, pp. 9–12.

[18] A. Elasser, M. Agamy, J. Sabate, R. Steigerwald, R. Fisher, and M. Harfman-Todorovic, "A comparative study of central and distributed MPPT architectures for megawatt utility and large scale commercial photovoltaic plants," in *Proc 36th Annu. Conf. IEEE Ind. Electron. Soc.*, 2010, pp. 2753–2758.

[19] B. Burger and R. Rüther, "Inverter sizing of grid-connected photovoltaic systems in the light of local solar resource distribution characteristics and temperature," *Solar Energy*, vol. 80, no. 1, pp. 32–45, 2006.

[20] S. Chen, P. Li, D. Brady, and B. Lehman, "The impact of irradiance time behaviors on inverter sizing and design," in *Proc. IEEE 12th Workshop Control Modeling Power Electron.*, 2010, pp. 1–5.

[21] S. I. Sulaiman, T. K. A. Rahman, and I. Musirin, "Design of grid-connected photovoltaic system using evolutionary programming," in *Proc. IEEE Int. Conf. Power Energy*, 2010, pp. 947–952.

[22] D. Weinstock and J. Appelbaum, "Optimal design of solar fields," in *Proc. 22nd Convention Electr. Electron. Eng.*, Israel, 2002, pp. 163–165.

[23] T. Kerekes, E. Koutroulis, S. Eyigün, R. Teodorescu, M. Katsanevakis, and D. Sera, "A practical optimization method for designing large PV plants," in *Proc. IEEE Int. Symp. Ind. Electron.*, 2011, pp. 2051–2056.

[24] A. M. Pavan, A. Mellit, and D. De Pieri, "The effect of soiling on energy production for large-scale photovoltaic plants," *Solar Energy*, vol. 85, no. 5, pp. 1128–1136, May 2011.

[25] A. Bidram, A. Davoudi, and R. S. Balog, "Control and circuit techniques to mitigate partial shading effects in photovoltaic arrays," *IEEE J. Photovoltaics*, vol. 2, no. 4, pp. 532–546, Oct. 2012.

[26] C. Deline, "Partially shaded operation of a grid-tied PV system," in *Proc. 34th IEEE Photovoltaic Specialists Conf.*, 2009, pp. 1268–1273.

[27] E. Lorenzo, *Solar Electricity—Engineering of Photovoltaic Systems*, 1st ed. New York: Taylor and Francis, 1994, pp. 87–99.

[28] M. García, J. A. Vera, L. Marroyo, E. Lorenzo, and M. Pérez, "Solar-tracking PV plants in Navarra: A 10 MW assessment," *Prog. Photovoltaics: Res. Appl.*, vol. 17, no. 5, pp. 337–346, 2009.

[29] U. K. W. Schwabe and P. M. Jansson, "Streamlining large scale photovoltaic arrays for utility interconnection," in *Proc. IEEE Bucharest PowerTech*, 2009, pp. 1–5.

[30] A. Kornelakis and E. Koutroulis, "Methodology for the design optimisation and the economic analysis of grid-connected photovoltaic systems," *IET Renewable Power Generation*, vol. 3, no. 4, pp. 476–492, 2009.

[31] Z. Michalewicz, *Genetic Algorithms + Data Structures = Evolution Programs*. New York: Springer-Verlag, 2nd ed., 1994, pp. 15–18.

[32] PVSYST Contextual Help | User's Guide, University of Geneva 1994-2010. (2011). [Online]. Available: www.pvsyst.com

Eftichios Koutroulis (M'10) was born in Chania, Greece, in 1973. He received the B.Sc., M.Sc., and Ph.D. degrees from the Department of Electronic and Computer Engineering, Technical University of Crete, Chania, Greece, in 1996, 1999, and 2002, respectively. His Ph.D. research focused on the area of power electronics and renewable energy sources.

He is currently an Assistant Professor with the Department of Electronic and Computer Engineering, Technical University of Crete. His research interests include power electronics (dc/ac inverters and dc/dc converters), the development of microelectronic energy management systems for renewable energy sources, and the design of photovoltaic and wind energy conversion systems.

Dezső Séra (M'09) received the B.Sc. and M.Sc. degrees in electrical engineering from the Technical University of Cluj, Cluj, Romania, in 2001 and 2002, respectively, the M.Sc. degree from the Department of Energy Technology (DET), Aalborg University, Aalborg, Denmark, in 2005, and the Ph.D. degree from the same department in 2009.

Since 2011, he has been an Associate Professor with DET, and since 2009, he has been the Coordinator of the Photovoltaic Systems Research Group with Aalborg University. His main interest includes photovoltaic energy generation, particularly modeling, diagnostics, MPPT, and control structures for photovoltaic systems.

Remus Teodorescu (F'12) received the Dipl. Ing. degree in electrical engineering from the Polytechnic University of Bucharest, Bucharest, Romania, in 1989 and the Ph.D. degree in power electronics from the University of Galati, Galați, Romania, in 1994.

In 1998, he joined the Department of Energy Technology, Power Electronics Section, Aalborg University, Aalborg, Denmark, where he currently works as a Professor. He has more than 200 IEEE papers published, one book (*Grid Converters for Photovoltaic and Wind Power Systems,* Hoboken, NJ: Wiley, 2011), and five patents. He is the Founder and Coordinator of the Green Power Laboratory, Aalborg University, focusing on the development and testing of grid converters for renewable energy systems. He is the Coordinator of Vestas Power Program, involving 10 Ph.D. students and Guest Professors in the areas of power electronics, power systems, and energy storage. His areas of interests include the design and control of power converters used in photovoltaics and wind power systems, grid integration with wind power, medium-voltage converters, high-voltage dc/flexible ac transmission systems, and energy storage.

Dr. Teodorescu a Past Associate Editor for IEEE TRANSACTIONS ON POWER ELECTRONICS LETTERS and a Chair of IEEE Danish joint IES/Power Electronics Society/Industry Applications Society chapter.

Tamás Kerekes (S'06–M'09) received the Electrical Engineer Diploma with specialization in electric drives and robots from the Technical University, Cluj, Romania, in 2002, and the M.Sc. degree in the field of power electronics and drives and the Ph.D. degree, in 2009, the topic of his Ph.D. program being "Analysis and modeling of transformerless PV inverter systems," both from Aalborg University, Aalborg, Denmark.

Since September 2012, he has been an Associate Professor with the Department of Energy Technology, Aalborg University, where he does research within grid-connected photovoltaic systems with special focus on design and control of photovoltaic inverters.

Markos Katsanevakis was born in Chania of Crete, Greece, in 1987. He received the B.Sc. degree in electrical engineering from the Technical Educational Institute of Crete, with orientation to power systems, in 2010. He is currently working toward the Master of Science degree in the field of electrical power systems and high-voltage engineering with the University of Aalborg, Aalborg, Denmark.

His research interests include the optimization of the energy production of photovoltaic (PV) plants, as well as identification and assessment of the effect of PV integration on the power system in terms of voltage stability, overcurrent protection, and loading of the grid components. He has also performed an Internship at ABB Corporate Research Center in Sweden in the area of photovoltaics.